

# Power Amplifier Design Fundamentals: More Notes from the Pages of History

By Andrei Grebennikov  
Bell Labs Ireland

This article is a thorough review of the behaviors of current, voltage and power that are the foundations for understanding power amplifier operation

In a previous excursion through the history of high-efficiency power amplifier design—published in *High Frequency Electronics*, Sept. 2008—it was found that new results very often

can represent long-forgotten ones. Sometimes those who were pioneering those technical ideas are undeservedly passed over, especially if it was long ago, perhaps almost a century.

In some cases, due to the difficulties with accessing the particular periodical publications, especially in different languages, the results are simply unknown. But it is always interesting to know how, where and when some technical idea or design principle first appeared. And, of course, history also should be learned in order not to repeat it. For example, most of the aspects of the power amplifier design basics described so long ago are still relevant and very useful nowadays in simplifying the entire design procedure, even with modern circuit design simulators.

## Operation Modes and Conduction Angle

As it was established at the end of the 1910s, the amplifier efficiency may reach quite high values when suitable adjustments of the grid and anode voltages are made [1]. With resistive load, the anode current is in phase with the grid voltage, whereas it leads with the capacitive load and it lags with the inductive load. On the assumption that the anode current and anode voltage both have sinusoidal variations, the maximum possible output of the amplifying device would be just half the DC supply power, or anode efficiency of

50%. However, by using a pulsed-shaped anode current, it is possible to achieve anode efficiency considerably in excess of 50%, potentially as high as 90%, by choosing the proper operation conditions.

By applying the proper negative bias voltage to the grid terminal to provide the pulsed anode current of different width, for angle  $\theta$  and angles greater than  $\theta$ , the anode current becomes equal to zero, where the double angle  $2\theta$  represents a conduction angle of the amplifying device [2]. In this case, a theoretical anode efficiency approaches 100% when the conduction angle, during which the anode current flows, reduces to zero starting from 50% which corresponds to the conduction angle of  $360^\circ$  or 100% duty cycle.

Generally, power amplifiers can be classified in three classes according to their mode of operation: *linear mode* when its operation is confined to the substantially linear portion of the active device characteristic curve; *critical mode* when the anode current ceases to flow, but operation extends beyond the linear portion up to the saturation and cutoff regions; and *nonlinear mode* when the anode current ceases to flow during a portion of each cycle, with a duration that depends on the grid bias [3]. When high efficiency is required, power amplifiers of the third class are employed since the presence of harmonics contributes to the attainment of high efficiencies. In order to suppress harmonics of the fundamental frequency to deliver a sinusoidal signal to the load, a parallel resonant circuit can be used in the load network which bypasses harmonics through a low impedance path and, by virtue of its resonance to the fundamental, receives energy at that frequency.

At the very beginning of 1930s, power amplifiers operating in the first two classes with 100% duty cycle were called Class A power amplifiers, whereas the power amplifiers operating in the third class with 50% duty cycle were assigned to Class B power amplifiers [4]. The Class A power amplifier with sinusoidal anode voltage and current waveforms can include a tuned or untuned load network with the load resistance  $R_L = V_m/I_m$ , where  $V_m$  and  $I_m$  are the anode voltage and current amplitudes, respectively. For an input cosine voltage, the operating point must be fixed at the middle point of the linear part of the device transfer characteristic which can be ideally represented by a piecewise-linear approximation. As a result, the output current is written as

$$i_a = I_a + I_m \cos \omega t \quad (1)$$

with the anode quiescent current  $I_a$  greater or equal to the anode current amplitude  $I_m$ . In this case, the output anode current contains only two components—DC and cosine—and the averaged current magnitude is equal to the quiescent current  $I_a$ . If the anode voltage amplitude  $V_m$  approaches the anode supply voltage  $V_a$  and the current amplitude  $I_m$  approaches the anode DC current  $I_a$  as a limit, the anode efficiency  $\eta = (V_m I_m / 2) / (V_a I_a)$  is equal to 50% for a sinusoidal output signal.

Class B power amplifiers had been defined as those which operate with a negative grid bias such that the anode current is practically zero with no excitation grid voltage, and in which the output power is proportional to the square of the excitation voltage [5]. In this case, no anode current flows during negative swing of the signal but the anode current is essentially proportional to the instantaneous value of the grid voltage on positive swings. As a result, the peak anode current is limited only by the emission, load resistance, and anode voltage.

Figure 1 shows the basic circuit schematic and voltage and current waveforms in a Class B operation with  $\theta = 90^\circ$  when the active device is biased to approximately the cutoff point. Here, the active device behaves as an ideal voltage-controlled current source having zero saturation resistance. The DC supply voltage  $V_a$  is applied to both plates of the DC-blocking capacitor having zero reactance at the operating frequency  $f_0$  and being constant during entire signal period, and  $R_L$  is the load resistor. By increasing the current ratio  $I_m / I_a$ , the anode efficiency can be increased, as follows from the expression for anode efficiency  $\eta$  for a Class A mode. This leads to a step-by-step nonlinear transformation of the current cosine waveform to a pulsed waveform when the magnitude of the anode current exceeds zero during only a part of the signal period. In this case, an active device (vacuum tube) is operated in the active region followed by operation in the cutoff region when the anode current is zero. In this case,

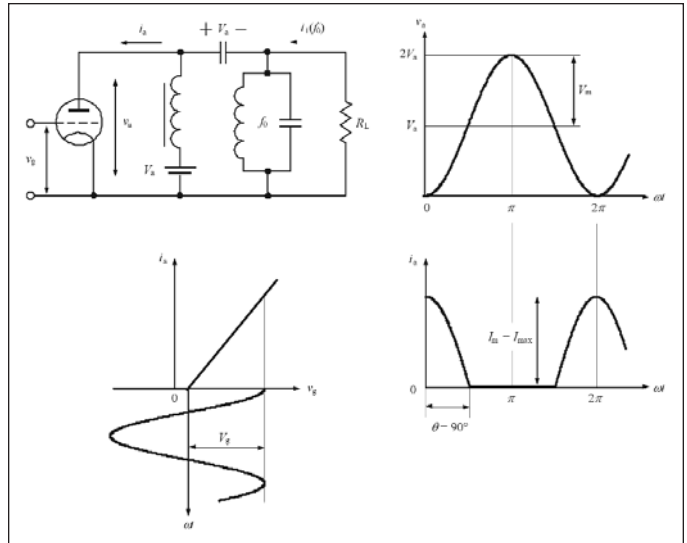


Figure 1 · Voltage and current waveforms in Class B operation mode.

the frequency spectrum at the device output will generally contain the second, third, and higher-order harmonics for different conduction angles. However, due to the high quality factor of the parallel resonant LC-circuit tuned to the fundamental frequency  $f_0$ , only the fundamental-frequency signal flows into the load, while the higher-order harmonic components are effectively short-circuited. Therefore, ideally the anode voltage represents a purely sinusoidal waveform with the voltage amplitude  $V \leq V_a$ . If the anode voltage amplitude  $V_m$  approaches the anode supply voltage  $V_a$  as a limit, then the anode efficiency  $\eta = 0.5(V_m I_m / 2) / (V_a I_m / \pi)$  is equal to  $\pi/4$  or 78.5% for half-cosine-wave output current [4].

Equation (1) for the output current can be rewritten through the ratio between the quiescent anode current  $I_a$  and the current amplitude  $I_m$  when  $i_a = 0$  as

$$\cos \theta = -\frac{I_a}{I_m} \quad (2)$$

As a result, the basic definitions for nonlinear operation modes of a power amplifier through half the conduction angle  $\theta$  can be introduced as

- when  $\theta > 90^\circ$ , then  $\cos \theta < 0$  and  $I_a > 0$  corresponding to Class AB operation
- when  $\theta = 90^\circ$ , then  $\cos \theta = 0$  and  $I_a = 0$  corresponding to Class B operation
- when  $\theta < 90^\circ$ , then  $\cos \theta > 0$  and  $I_a < 0$  corresponding to Class C operation.

Class C power amplifiers had been defined as those that operate with a negative grid bias more than suffi-

cient to reduce the anode current to zero with no excitation grid voltage, and in which the output power varies as the square of the anode voltage between limits [5]. The main distinction between Class B and Class C is in the duration of the output current pulses which are shorter for Class C when the active device is biased beyond the cutoff point.

The periodic pulsed output current  $i_a(\omega t)$  can be represented as a Fourier series expansion

$$i_a(\omega t) = I_o + I_1 \cos \omega t + I_2 \cos 2\omega t + I_3 \cos 3\omega t \dots \quad (3)$$

where the DC, fundamental-frequency, and  $n$ th harmonic components are calculated by

$$I_o = \frac{1}{2\pi} \int_{-\theta}^{\theta} I_m (\cos \omega t - \cos \theta) d\omega t = \gamma_0(\theta) I_m \quad (4)$$

$$I_1 = \frac{1}{\pi} \int_{-\theta}^{\theta} I_m (\cos \omega t - \cos \theta) \cos \omega t d\omega t = \gamma_1(\theta) I_m \quad (5)$$

$$I_n = \frac{1}{\pi} \int_{-\theta}^{\theta} I_m (\cos \omega t - \cos \theta) \cos n\omega t d\omega t = \gamma_n(\theta) I_m \quad (6)$$

where  $\gamma_n(\theta)$  are called the  $n$ th-harmonic coefficients of expansion of the output current waveform or the  $n$ th-harmonic current coefficient [6, 7]. They can be analytically defined as

$$\gamma_o(\theta) = \frac{1}{\pi} (\sin \theta - \theta \cos \theta) \quad (7)$$

$$\gamma_1(\theta) = \frac{1}{\pi} \left( \theta - \frac{\sin 2\theta}{2} \right) \quad (8)$$

$$\gamma_n(\theta) = \frac{1}{\pi} \left[ \frac{\sin(n-1)\theta}{n(n-1)} - \frac{\sin(n+1)\theta}{n(n+1)} \right] \quad (9)$$

where  $n = 2, 3, \dots$ . As a result, for a Class B mode with  $\theta = 90^\circ$  corresponding to a half-cosine anode current waveform, the odd-harmonic current coefficients  $\gamma_n(\theta)$  are equal to zero, as it follows from Eq. (9) for odd  $n$ . It should be noted that, for the device transfer characteristic, which can be ideally represented by a square-law approximation, the odd-harmonic current coefficients  $\gamma_n(\theta)$  are not equal to zero in this case, although there is no significant difference between the square-law and linear cases [8]. To obtain the maximum anode efficiency in Class C, the active device should be biased (negative) considerably past the cutoff point to provide the sufficiently low conduction angles [9].

From Eqs. (4), (5), (7), and (8) it follows that the ratio of the fundamental-frequency component of the anode current to the DC current is a function of  $\theta$  only,

$$\frac{I_1}{I_o} = \frac{\theta - \sin \theta \cos \theta}{\sin \theta - \theta \cos \theta} \quad (10)$$

which means that, if the operating angle is maintained constant, the fundamental component of the anode current will replicate linearly to the variation of the DC current, thus providing the linear operation of the Class C power amplifier when DC current is directly proportional to the grid voltage [10].

### Load Line and Output Impedance

The graphical method of laying down a *load line* on the family of the static curves representing anode current versus anode voltage for various grid potentials was already well known in the 1920s [11]. If an active device is connected in a circuit in which the anode load is a pure resistance, the performance may be analyzed by drawing the load line where the lower end of the line represents the anode supply voltage and the slope of the line is established by the load resistance, that is, the resistance is equal to the value of the intercept on the voltage axis divided by the value of the intercept on the current axis.

In Class A, the output voltage  $v_a$  across the device anode (collector or drain) represents a sum of the DC supply voltage  $V_a$  and cosine voltage across the load resistance  $R_L$ . Consequently, the greater output current  $i_a$ , the greater voltage across the load resistance  $R_L$  and the smaller output voltage  $v_a$ . Thus, for a purely real load impedance ( $Z_L = R_L$ ) the anode voltage  $v_a$  is shifted by  $180^\circ$  relative to the grid voltage  $v_g$  and can be written as

$$v_m = V_a + V_m \cos(\omega t + 180^\circ) = V_a - V_m \cos \omega t \quad (11)$$

Substituting Eq. (1) into Eq. (11) yields

$$v_a = V_a - (i_a - I_o) R_L \quad (12)$$

where  $R_L = V_m/I_m$  is the load resistance. In this case, the power dissipated in the load and the power dissipated in the tube is equal when  $V_a = V_m$ , and the load resistance  $R_L$  is equal to the tube output resistance  $R_{out}$  [5].

Equation (12) can be rewritten in the form

$$i_m \left( I_a + \frac{V_a}{R_L} \right) - \frac{v_a}{R_L} \quad (13)$$

which determines a linear analytical dependence of the anode current versus anode voltage. In practical applications, because of the device nonlinearities, it is necessary to connect a parallel *LC*-circuit with resonant frequency equal to the operating frequency to suppress any possible harmonic components.

In a pulsed operation mode (Classes AB, B, or C), since the parallel *LC*-circuit is tuned to the fundamental fre-

quency, ideally the voltage across the load resistor  $R_L$  represents a cosine waveform. In this case, the relationship between the anode current  $i_a$  and voltage  $v_a$  during a time period of  $-\theta \leq \omega t < \theta$  can be expressed using Eqs. (2) and (11) as

$$i_a = \left( I_a + \frac{V_a}{\gamma_1 R_L} \right) - \frac{v_a}{\gamma_1 R_L} \quad (14)$$

where the fundamental current coefficient  $\gamma_1$  as a function of  $\theta$  is determined by Eq. (8) and the load resistance is defined by  $R_L = V_m/I_1$  where  $I_1$  is the fundamental-frequency current amplitude. Equation (14) determining the dependence of the anode current on the anode voltage for any values of conduction angle in the form of a straight line function with different slope angles  $\beta = \tan^{-1}(1/\gamma_1 R_L)$  is called the load line of the active device in a general form. For a Class A operation mode with  $\theta = 180^\circ$  when  $\gamma_1 = 1$ , Eq. (14) becomes identical to Eq. (13). The formulas for the amplitudes of the harmonic components can be obtained in terms of points taken from the load line on the anode voltage-current characteristics at equally spaced intervals of grid voltage [12].

The load resistance  $R_L$  for the active device as a function of  $\theta$  which is required to terminate the device output in order to deliver maximum output power to the load can be written in a general form as

$$R_L(\theta) = \frac{V_m}{\gamma_1(\theta) I_m} \quad (15)$$

which is equal to the tube equivalent output resistance  $R_{out}$  at the fundamental frequency [5]. The term “equivalent” means that this is not a real physical tube resistance as in a Class A mode, but its equivalent output resistance, the value of which determines the optimum load, which should terminate the tube output to deliver maximum fundamental-frequency output power. The equivalent output resistance is calculated as a ratio between the amplitudes of the anode cosine voltage and fundamental-frequency anode current component, which depends on the angle  $\theta$ . In a Class B mode when  $\theta = 90^\circ$  and  $\gamma_1 = 0.5$ , the load resistance  $R_L^B$  is defined as  $R_L^B = 2V_a / I_{max}$ .

Class B power amplifiers are often driven hard enough to cause the active devices to enter saturation during a portion of each RF cycle, resulting in a depression in the top part of the cosine anode waveform. Similar results can be achieved by increasing the value of  $R_L$  when the load line is characterized by smaller slope angle  $\beta$ . The anode current waveform becomes asymmetrical for the complex load, the impedance of which is composed of the load resistance and capacitive or inductive reactance. In this case, the Fourier expansion of the pulsed anode current given by Eq. (3) includes a particular phase for

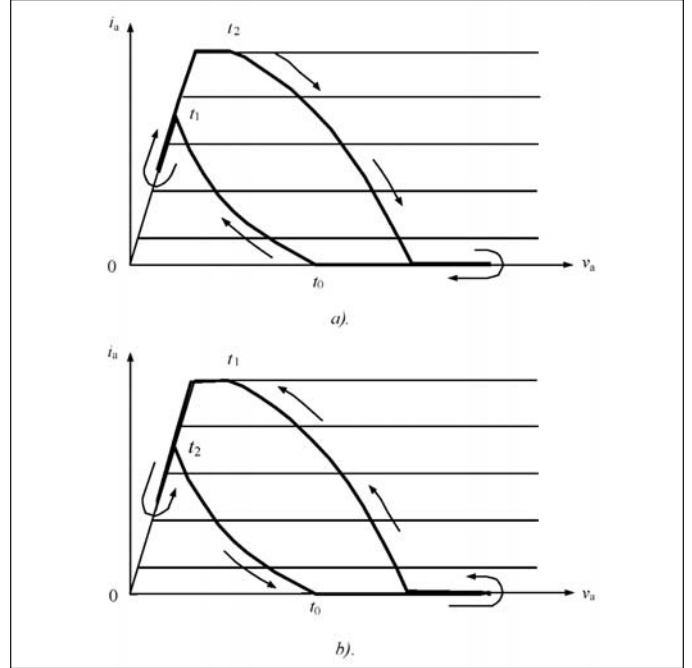


Figure 2 · Load lines for (a) inductive and (b) capacitive load impedances.

each harmonic components. Then, generally the anode voltage of the active device is written as

$$v_a = V_a - \sum_{n=1}^{\infty} I_n |Z_n| \cos(n\omega t + \phi_n) \quad (16)$$

where  $I_n$  is the amplitude of  $n$ th output current harmonic component,  $|Z_n|$  is the magnitude of the load network impedance at  $n$ th output current harmonic component, and  $\phi_n$  is the phase of  $n$ th output current harmonic component. Assuming that  $Z_n$  is zero for  $n = 2, 3, \dots$ , which is possible for a resonant load network having negligible impedance at any harmonic component except the fundamental, Eq. (16) can be rewritten as

$$v_a = V_a - I_1 |Z_1| \cos(\omega t + \phi_1) \quad (17)$$

As a result, for the inductive load impedance, the depression in the anode current waveform reduces and moves to the left-hand side of the waveform, whereas the capacitive load impedance causes the depression to deepen and shift to the right-hand side of the anode current waveform [13]. This effect can simply be explained by the different phase conditions for fundamental and higher order harmonic components composing the anode current waveform and is illustrated by the different load lines for (a) inductive and (b) capacitive load impedances shown in Figure 2. Note that now the load line represents the two-dimensional curve with a complicated behavior.

### Power Gain and Output Matching

In order to extract the maximum power from a generator, it is well known fact that the external load should have a vector value which is conjugate of the internal impedance of the source [14]. The power delivered from a generator to a load, when matched on this basis, will be called the available power of the generator [15]. In this case, the power gain of the four-terminal network is defined as the ratio of the power delivered to the load impedance connected at the output terminals to the power available from the generator connected to the input terminals, usually measured in decibels, and this ratio is called “power gain” irrespective of whether it is greater or less than one [16, 17].

Figure 3 shows the basic block schematic of the single-stage power amplifier circuit which includes an active device, an input matching circuit to match with the source impedance, and an output matching circuit to match with the load impedance. Generally, the two-port active device can be characterized by a system of immittance  $W$ -parameters, which is any system of impedance  $Z$ -parameters, hybrid  $H$ -parameters, or admittance  $Y$ -parameters [18, 19]. The input and output matching circuits transform the source and load immittances  $W_S$  and  $W_L$  into specified values between points 1-2 and 3-4, respectively, by means of which the optimal design operation mode of the power amplifier is realized.

The transducer power gain  $G_T$  defined as the ratio of the power delivered to the load immittance  $W_L$  to the power available from the source having an immittance  $W_S$  can be expressed in terms of the immittance  $W$ -parameters as

$$G_T = \frac{4|W_{21}|^2 \operatorname{Re} W_S \operatorname{Re} W_L}{|(W_{11} + W_S)(W_{22} + W_L) - W_{12}W_{21}|^2} \quad (18)$$

The operating power gain  $G_P$  defined as the ratio of power delivered to the load immittance  $W_L$  to the power delivered to the input port of the active device with an immittance  $W_{in}$  can be expressed in terms of the immittance  $W$ -parameters as

$$G_P = \frac{|W_{21}|^2 \operatorname{Re} W_L}{|W_{22} + W_L|^2 \operatorname{Re} W_{in}} \quad (19)$$

where the input and output immittances  $W_{in}$  and  $W_{out}$  are defined as

$$W_{in} = W_{11} = \frac{W_{12}W_{21}}{W_{22} + W_L} \quad (20)$$

$$W_{out} = W_{22} = \frac{W_{12}W_{21}}{W_{11} + W_S} \quad (21)$$

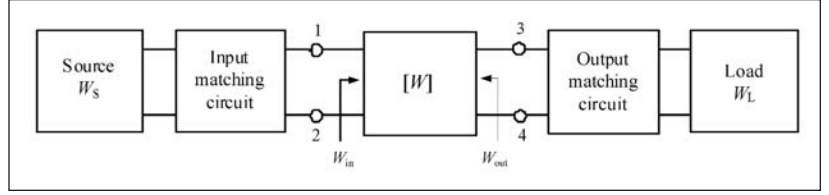


Figure 3 · Generalized single-stage power amplifier circuit.

The operating power gain  $G_P$  does not depend on the source parameters and characterizes only the effectiveness of the power delivery from the input port of the active device to the load. This power gain helps to evaluate the gain property of a multistage amplifier when the overall operating power gain  $G_{P(\text{total})}$  is equal to the product of each stage  $G_P$ . The transducer power gain  $G_T$  includes an assumption of conjugate matching of both the load and the source. In this case, the denominator of Eq. (18) becomes minimal since the reactive parts of the imaginary parts of the device input and output impedances are compensated for, thus resulting in a maximum available transducer power gain  $G_T$ .

It should be noted that Eqs. (18) and (19) are given in general immittance forms without indication of whether they are used in a small-signal or large-signal application. In the latter case, this only means that the device immittance  $W$ -parameters are fundamentally averaged over large signal swing across the device equivalent circuit parameters and that the conjugate-matching principle is valid in both the small-signal application and the large-signal application where the optimum equivalent device output resistance is matched to the load resistance and the effect of the device output reactance is eliminated by the conjugate reactance of the load network.

Note that the load resistance  $R_L$  defined by the general load-line dependence given by Eq. (14) is a ratio of the output cosine voltage and fundamental-frequency current amplitudes which in turn determines the optimum device equivalent output resistance when maximum fundamental-frequency output power is delivered to the load, and load line represents only a graphical interpretation of real physical process. Therefore, it is generally incorrect to introduce separately the concepts of the gain match with respect to the linear power amplifiers only and the power match in nonlinear power amplifier circuits since the maximum large-signal power gain being a function of the angle  $\theta$  corresponds to the maximum fundamental-frequency output power delivered to the load due to large-signal conjugate output matching. It is very important to provide a conjugate matching at both input and output device ports to achieve maximum power gain in a large-signal mode. It also implies an efficiency match for the specified conduction angle since the maximum achievable anode (collector or drain) efficiency is a function of the

angle  $\theta$  as well. In a Class A mode, the maximum small-signal power gain ideally remains constant regardless of the output power level.

The transistor characterization in a large-signal mode can be done based on equivalent quasi-harmonic nonlinear approximation under the condition of sinusoidal port voltages [20]. In this case, the large-signal impedances are generally determined in the following manner. The designer tunes the load network (often by trial and errors) to maximize the output power to the required level using a particular transistor at a specified frequency and supply voltage. Then, the transistor is removed from the circuit and the impedance seen by the collector is measured at the carrier frequency. The complex-conjugate of the measured impedance then represents the equivalent large-signal output impedance of the transistor at that frequency, supply voltage, and output power. Similar design process is used to measure the input impedance of the transistor and to maximize power-added efficiency of the power amplifier.

To deliver maximum power to the load, it is necessary to use some impedance matching network which can modify the load as viewed from the generator [14]. The design of reactance networks to connect a resistive load efficiently to a source of power can be carried out most conveniently by the theory of image impedances. In this case, if the image impedances of such a network are pure resistances and it is connected between a generator and a load whose impedances are equal to these image impedances, the impedances will match at both junctions. Under these conditions, with an assumption of pure reactances of the arms of the connecting network, no power will dissipate during transmission and so the maximum power will be delivered to the load. If the terminating impedances are not pure resistances, they can be made so at any single frequency by placing additional reactance in series. Such reactance networks can provide not only for high efficiency but can also attenuate undesired harmonics. A variety of configurations can be designed to accomplish the desired result. Both  $T$ -type and  $\pi$ -type configurations are most popular for matching networks, depending on convenience of the circuit implementation and particular application technology. They can be implemented in both low-pass and high-pass topologies.

### Load Pull Characterization

*Load pull* is a computer-controlled technique for large-signal characterization of microwave power transistors used to map contours of constant power and efficiency on a Smith chart for dynamic matching of both input and output circuits. This was originally developed for the interstage matching between a varactor multiplier and a transistor power stage, and then successfully applied to the broadband optimization of Class A and Class C tran-

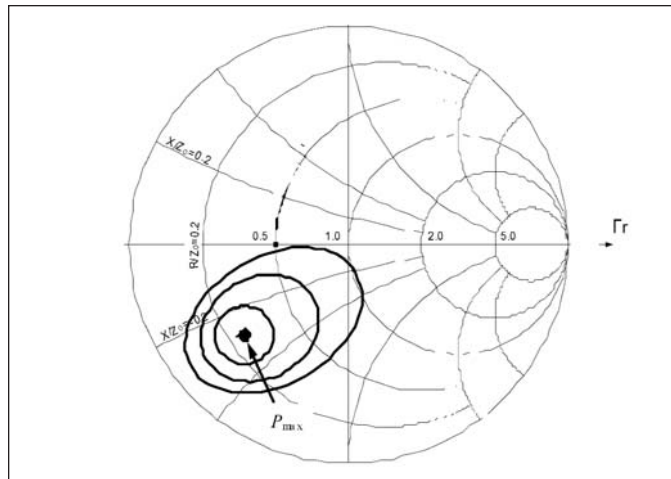


Figure 4 · Constant-power load-pull contours.

sistor power amplifiers [21, 22]. The power-load contours consist of a series of curves on a Smith chart representing constant output power, approaching the point of maximum output power, as shown in Figure 4. When drawn at several frequencies over the band of interest, they represent loci of required output impedance for various output power levels. If constant efficiency contours are overlaid on the constant power contours, the efficiency is also known at each of the load impedances.

A power transistor operated in the Class C mode has an output equivalent circuit which is represented by a nonlinear multiharmonic current source and a nonlinear reactance. To obtain maximum output power, the load impedance must produce the maximum current and voltage swing. The relationship between the required load impedance and nonlinear output impedance determines the shape of the power-load contour which can vary with input drive level. For low drive levels, the contour is almost elliptical. As the drive level increases toward the point where the transistor current saturates, the power-load contour expands into a circle with a constant transmission loss circle [23]. To get a variable load, in addition to the traditional passive-network technique with variable elements, an active load-pull characterization can be used where the reflection coefficient is obtained using an auxiliary signal derived from the same test generator to inject into the output port [24, 25]. One of the advantages of this technique lies in the inherent simplicity of the calibration procedure necessary to correct the transmission-line losses in the measurement system. However, its accuracy critically depends on the effective directivities of the directional couplers in the system [26]. Independent tuning of the fundamental frequency and its second harmonic had become possible by using a scheme with frequency-selective tuners [27].

Generally, tuning with a load-pull system (mechanical

or fully automatic) is a very complicated procedure, especially we must take into account several harmonics of the fundamental frequency. Besides, it can only give the optimum input and output impedances, as are usually incorporated in the datasheet for power transistors for specified output power, supply voltage and frequency range. In a monolithic implementation, however, this is difficult to physically realize and can be done based on the load-pull setup incorporated into the simulation tool. But, in all cases, the measurement should be followed by the subsequent load-network design with real elements. Therefore, in most cases where the device nonlinear model is available, the device equivalent output circuit can be represented by the output admittance where the equivalent output resistance can be estimated from Eq. (15) for fixed conduction angle and supply voltage equal ideally to the cosine voltage amplitude (the corresponding device saturation voltage can be subtracted). For example, in a Class B mode with  $\theta = 90^\circ$ , it is written as  $R_L = V_a/I_1 = V_a^2/2P_{out}$ , where  $P_{out}$  is the maximum fundamental-frequency power delivered to the load, and the output shunt reactance is represented by the sum of the output and feedback capacitances.

### Next Month

This article concludes next month with discussions of stability and the effects of higher-order harmonics.

### Author Information

Andrei Grebennikov received the MSc degree in electronics from Moscow Institute of Physics and Technology, and the Ph.D. degree in radio engineering from Moscow Technical University of Communications and Informatics. He can be reached by e-mail at: grandrei@iee.org

### References

1. J. H. Morecroft and H. T. Friis, "The Vacuum Tubes as a Generator of Alternating-Current Power," *Trans. AIEE*, vol. 38, pp. 1415-1444, Oct. 1919.
2. D. C. Prince, "Vacuum Tubes as Power Oscillators, Part I," *Proc. IRE*, vol. 11, pp. 275-313, June 1923.
3. A. A. Oswald, "Power Amplifiers in Trans-Atlantic Radio Telephony," *Proc. IRE*, vol. 13, pp. 313-324, June 1925.
4. L. E. Barton, "High Audio Power from Relatively Small Tubes," *Proc. IRE*, vol. 19, pp. 1131-1149, July 1931.
5. C. E. Fay, "The Operation of Vacuum Tubes as Class B and Class C Amplifiers," *Proc. IRE*, vol. 20, pp. 548-568, Mar. 1932.
6. P. H. Osborn, "A Study of Class B and C Amplifier Tank Circuits," *Proc. IRE*, vol. 20, pp. 813-834, May 1932.
7. A. I. Berg, *Theory and Design of Vacuum-Tube Generators* (in Russian), Moskva: GEI, 1932.
8. F. E. Terman and J. H. Ferns, "The Calculation of Class C Amplifier and Harmonic Generator Performance of Screen-Grid and Similar Tubes," *Proc. IRE*, vol. 22, pp. 359-373, Mar. 1934.
9. L. B. Hallman, "A Fourier Analysis of Radio-Frequency Power Amplifier Wave Forms," *Proc. IRE*, vol. 20, pp. 1640-1659, Oct. 1932.
10. W. L. Everitt, "Optimum Operating Conditions for Class C Amplifiers," *Proc. IRE*, vol. 22, pp. 152-176, Feb. 1934.
11. C. E. Kilgour, "Graphical Analysis of Output Tube Performance," *Proc. IRE*, vol. 19, pp. 42-50, Jan. 1931.
12. D. C. Espley, "The Calculation of Harmonic Production in Thermionic Valves with Resistive Load," *Proc. IRE*, vol. 21, pp. 1439-1446, Oct. 1933.
13. V. I. Kaganov, *Transistor Radio Transmitters* (in Russian), Moskva: Energiya, 1976.
14. W. L. Everitt, "Output Networks for Radio-Frequency Power Amplifiers," *Proc. IRE*, vol. 19, pp. 725-737, May 1931.
15. H. T. Friis, "Noise Figure of Radio Receivers," *Proc. IRE*, vol. 32, pp. 419-422, July 1944.
16. S. Roberts, "Conjugate-Image Impedances," *Proc. IRE*, vol. 34, pp. 198-204, Apr. 1946.
17. S. J. Haefner, "Amplifier-Gain Formulas and Measurements," *Proc. IRE*, vol. 34, pp. 500-505, July 1946.
18. R. L. Pritchard, "High-Frequency Power Gain of Junction Transistors," *Proc. IRE*, vol. 43, pp. 1075-1085, Sept. 1955.
19. A. R. Stern, "Stability and Power Gain of Tuned Power Amplifiers," *Proc. IRE*, vol. 45, pp. 335-343, Mar. 1957.
20. L. S. Houselander, H. Y. Chow, and R. Spense, "Transistor Characterization by Effective Large-Signal Two-Port Parameters," *IEEE J. Solid-State Circuits*, vol. SC-5, pp. 77-79, Apr. 1970.
21. E. F. Belohoubek, A. Rosen, D. M. Stevenson, and A. Presser, "Hybrid Integrated 10-Watt CW Broad-Band Power Source at S Band," *IEEE J. Solid-State Circuits*, vol. SC-4, pp. 360-366, Dec. 1969.
22. A. Presser and E. F. Belohoubek, "1-2 GHz High Power Linear Transistor Amplifier," *RCA Rev.*, vol. 33, pp. 737-751, Dec. 1972.
23. J. M. Cusack, S. M. Perlow, and B. S. Perlman, "Automatic Load Contour Mapping for Microwave Power Transistors," *IEEE Trans. Microwave Theory Tech.*, vol. MTT-12, pp. 1146-1152, Dec. 1974.
24. Y. Takayama, "A New Load-Pull Characterization Method for Microwave Power Transistors," *1976 IEEE MTT-S Int. Microwave Symp. Dig.*, pp. 218-220.
25. G. P. Bava, U. Pisani, and V. Pozzolo, "Active Load Technique for Load-Pull Characterization at Microwave Frequencies," *Electronics Lett.*, vol. 18, pp. 178-180, Feb. 1982.
26. C. Rauscher and H. A. Willing, "Simulation of Nonlinear Microwave FET Performance Using a Quasi-Static Model," *IEEE Trans. Microwave Theory Tech.*, vol. MTT-27, pp. 834-840, Oct. 1979.
27. R. B. Stancliff and D. D. Poulin, "Harmonic Load-Pull," *1979 IEEE MTT-S Int. Microwave Symp. Dig.*, pp. 185-187.